

## Supporting Information

# Intermetallic Differences at CdS-Metal (Ni, Pd, Pt, and Au) Interfaces: From Single-atom to Subnanometer Metal Clusters

S.S. Gupta and M.A. van Huis\*

*Soft Condensed Matter, Debye Institute for Nanomaterials Science, Utrecht University,  
Princetonplein 5, 3584 CC Utrecht, The Netherlands*

E-mail: M.A.vanHuis@uu.nl

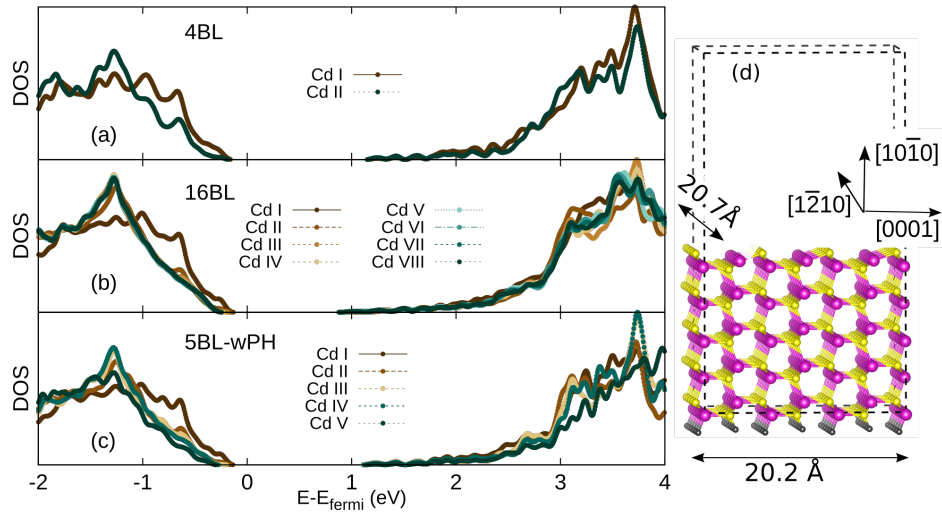


Figure S1: Figure (a)-(c) show the layer-wise averaged density of states of Cd-atoms, where I refers to the topmost layer and BL refers to the bilayers comprising the slab. All the energies are referenced from the respective Fermi energies of the calculations. Panel (a) and (b) correspond to unpassivated  $(10\bar{1}0)$  surface unit slabs of thickness 4BL and 16BL, respectively. Panel (c) corresponds to a pseudohydrogen passivated 5BL slab (5BL-wPH, shown in the schematic on the right) which is used in our study for the deposition of single-atom and clusters. A comparison of (c) with (b) shows that for 5BL-wPH slab, all the layers resemble the valence band region of the 16BL model, except from the bottom-most layer, where the explicit passivation occurs.

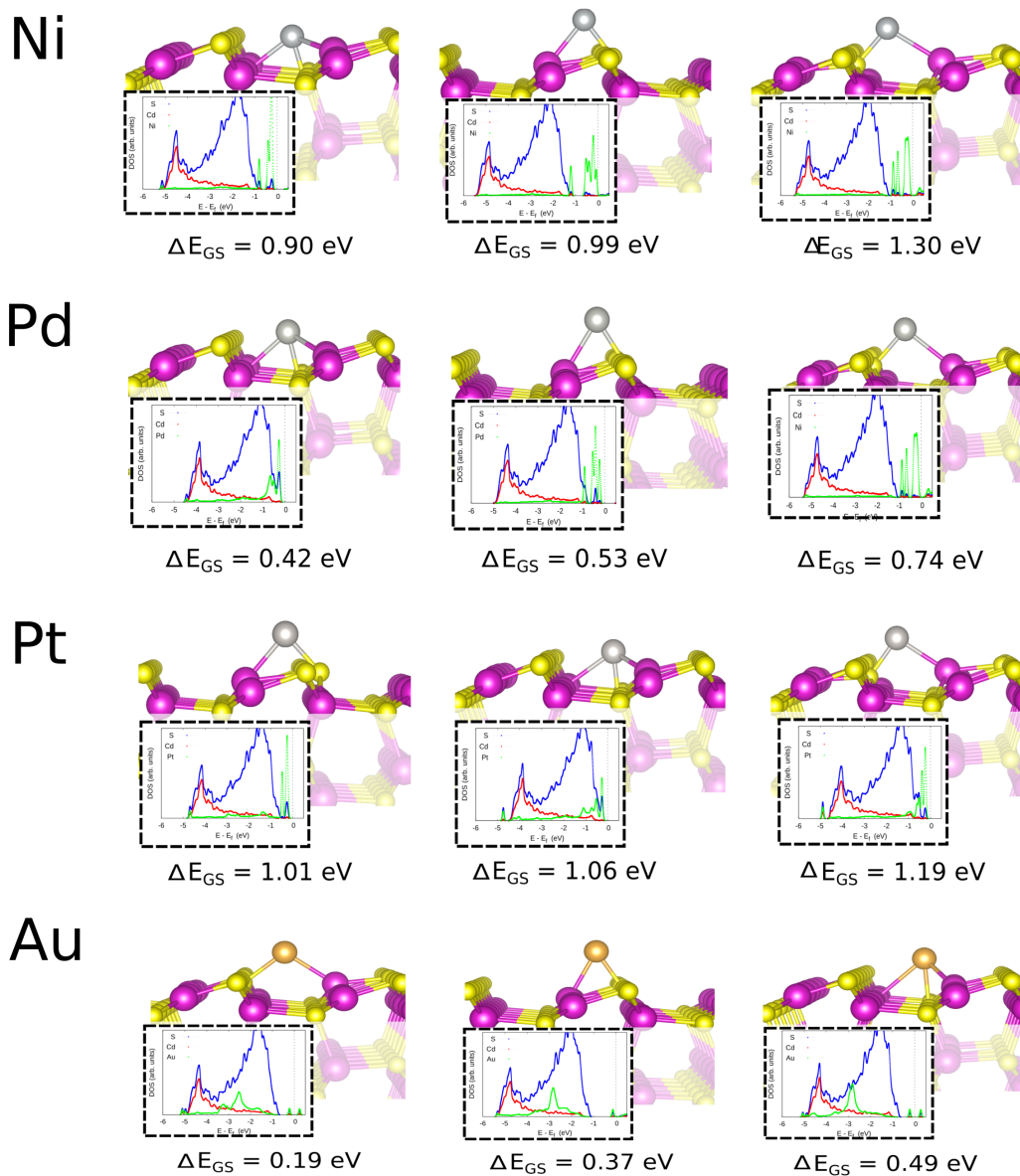


Figure S2: Metastable sites for Ni<sub>1</sub> in the decreasing order of  $E_{adh}$ , from left to right

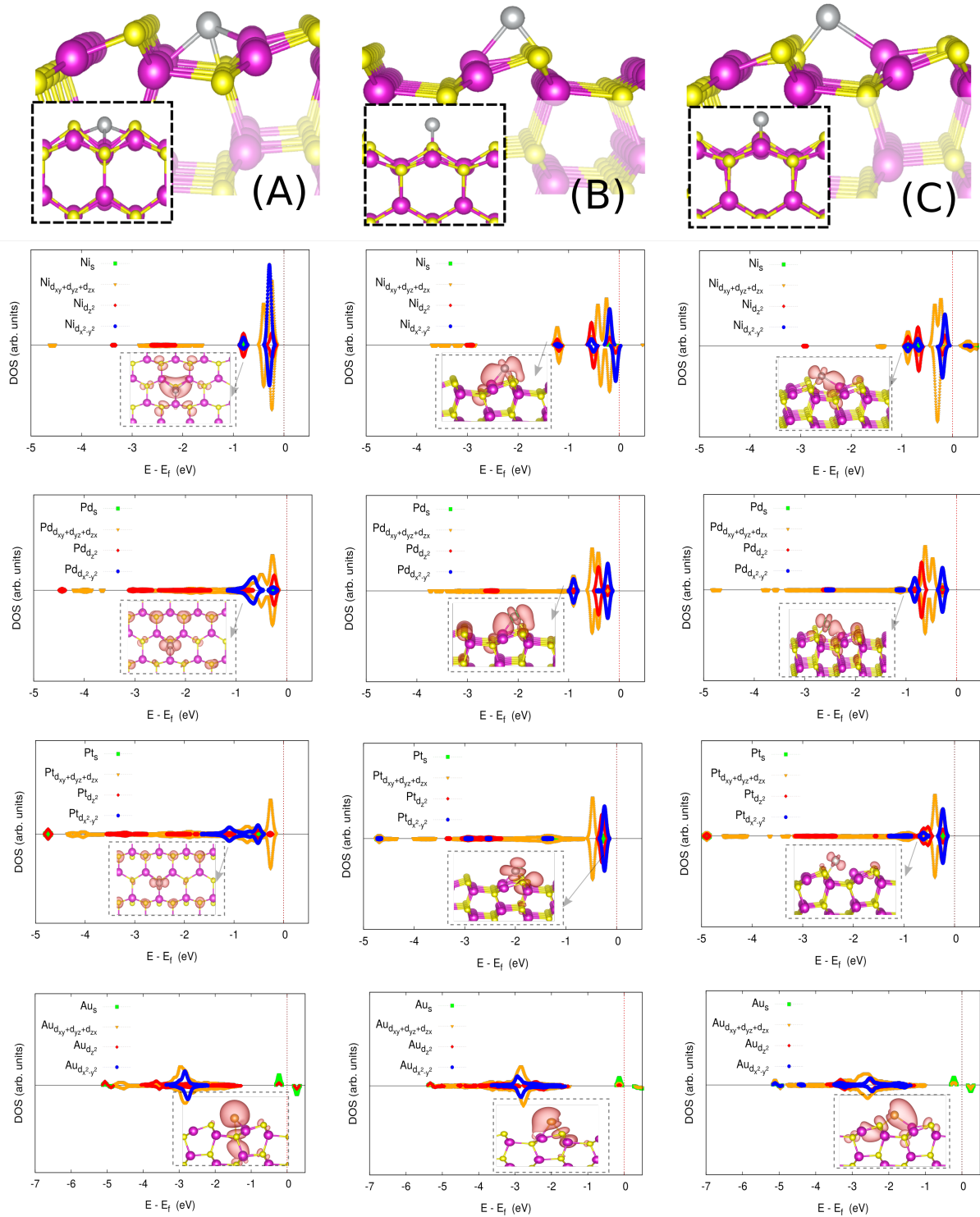


Figure S3: (A), (B) and (C) represent the metastable single-atom adsorption geometries over CdS (10 $\bar{1}$ 0). The panels below show their respective density of states for different metal-atoms. The insets show the partial charge density of the bonding/antibonding states indicated in the figure.

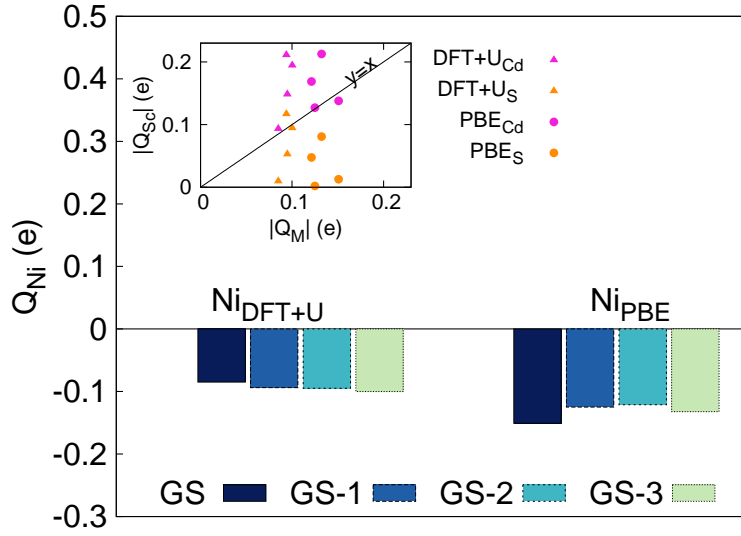


Figure S4: The bar plots shows the bader charge on the single-atom adsorption cases of Ni, with and without DFT+U scheme. The  $U_{Ni} = 3.5$  eV was taken from the literature. The GS- $i$  ( $i = 1 \rightarrow 3$ ) refers to the metal-stable sites with decreasing adhesion energy from the ground state (GS). The inset shows the magnitude of sum of bader charges on the surface Cd and S, and compared with the magnitude of Bader charge on the Ni atom.

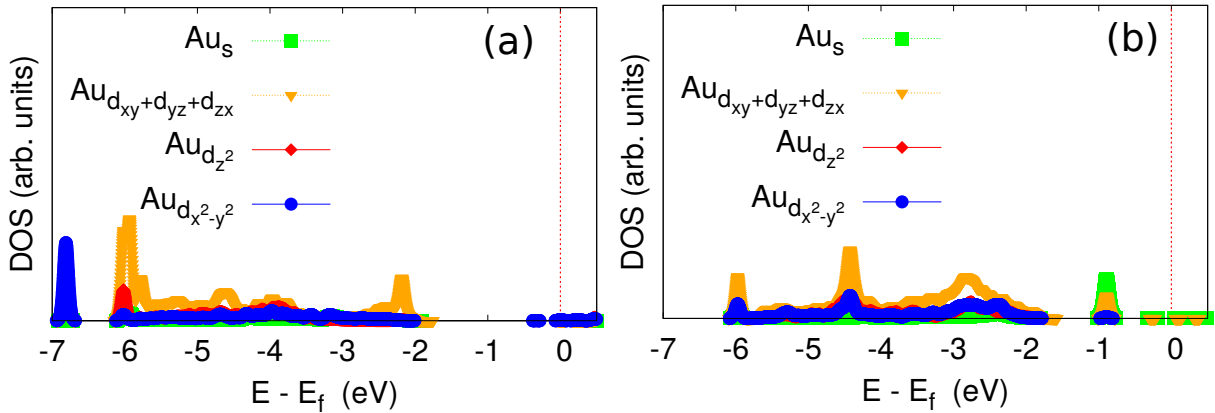


Figure S5: (a) and (b) show the PDOS of the adsorbed  $Au_1$  for GS and GS - 1 configurations, respectively.

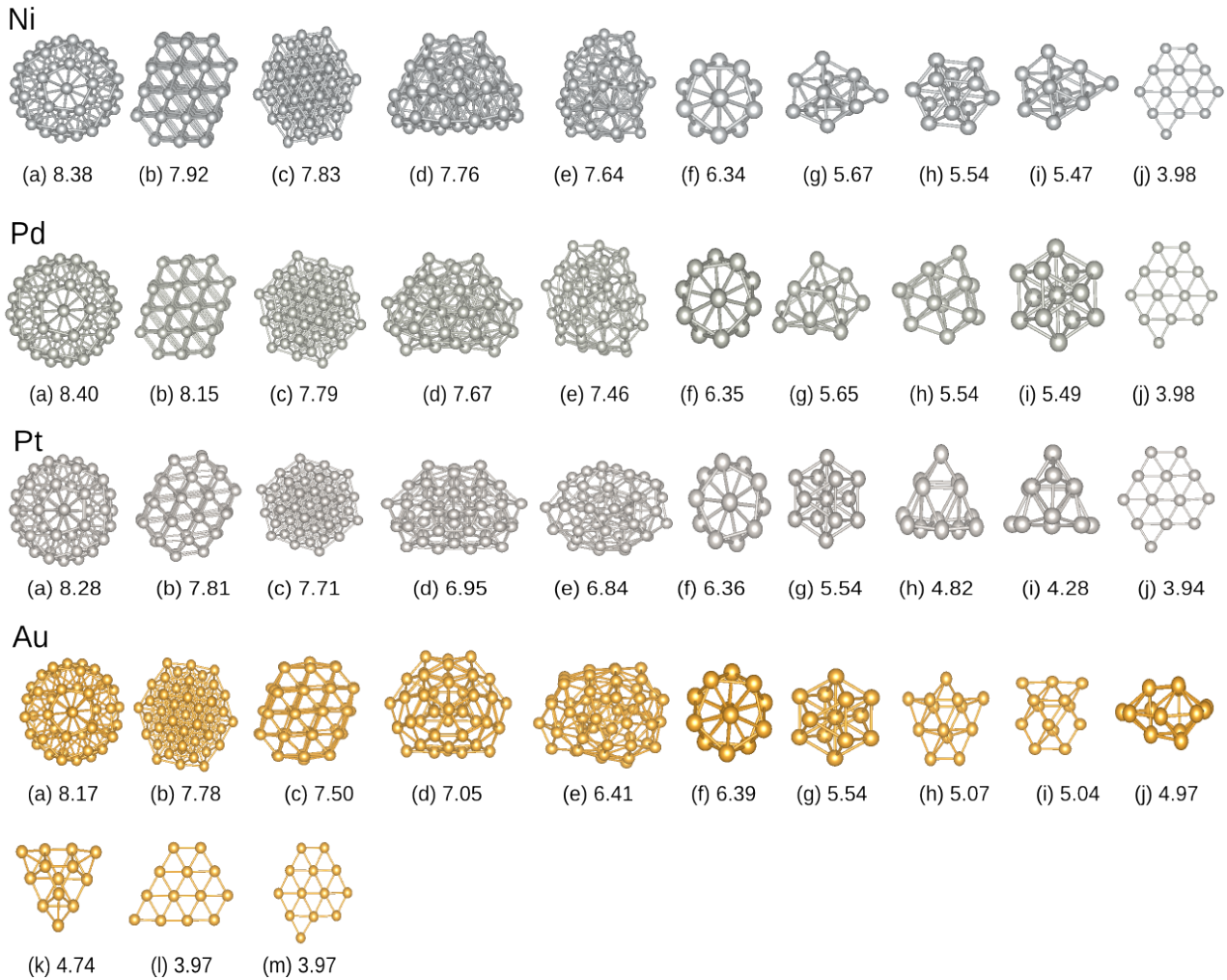


Figure S6: Figures shows all the isolated gas-phase clusters studied, before making a selection for CdS-deposition. The clusters are arranged (left to right) in the decreasing order of ECN, written below them. The underlined clusters were deposited over CdS surface in this study. These clusters have been adopted from the literature, as follows:

**Ni:** (a) ICO55 (Icosahedron), (b) FCC55; Pd FCC-fragment reported by Da Silva et. al.,<sup>1</sup> (c) Cuboctahedron55, (d) CCD55; Cd geometry for Gupta potential reported by Doye et. al.,<sup>2</sup> (e) DRC55; Pt distorted reduced core geometry reported by Da Silva et. al.,<sup>1,3</sup> (f) ICO13, (g) GS13, Ni geometry reported by Chou et. al.<sup>4</sup> (h) Cubocahedron13, (i) Ni13 geometry from Da Silva et. al.,<sup>5</sup> (j) PLA13; Au geometry reported by Chou et. al.<sup>4</sup>

**Pd:** (a)-(f) same references as mentioned for Ni clusters, (h) GS13; Pd bilayer geometry reported by Pelzer et. al.,<sup>6</sup> (i) Cubocahedron13, (j) PLA13; Au geometry reported by Chou et. al.<sup>4</sup>

**Pt:** (a)ICO55 (b) FCC55; Pd FCC-fragment reported by Da Silva et. al.,<sup>1</sup> (c) Cuboctahedron55, (d) CCD55; Cd geometry for Gupta potential reported by Doye et. al.<sup>2</sup> (e) DRC55; Pt distorted reduced core geometry reported by Da Silva et. al.,<sup>1,3</sup> (f) ICO13, (g) Cubocahedron13, (h) GS13; Pt geometry reported by Sun et. al.,<sup>7</sup> (i) Pt geometry reported by Chou et. al.,<sup>4</sup> (j) PLA13; Au geometry reported by Chou et. al.<sup>4</sup>

**Au:** (a)ICO55 (b) Cuboctahedron55, (c) FCC55; Pd FCC-fragment reported by Da Silva et. al.<sup>1</sup> (d) CCD55; Cd geometry for Gupta potential reported by Doye et. al.<sup>2</sup> (e) DRC55; Pt distorted reduced core geometry reported by Da Silva et. al.,<sup>3</sup> (f) ICO13, (g) 13Cubocahedron, (h)-(i) Au<sub>13</sub>-I, Au<sub>13</sub>-II geometries reported by Furche et. al.,<sup>8</sup> (j) 3D structure reported by Da Silva et. al.,<sup>5</sup> (k) GS13; 3D structure, Au<sub>13</sub>-III, reported by Furche et. al.<sup>8</sup> (l) Au geometry reported by Munoz et. al.<sup>9</sup> (m) PLA13; Au geometry reported by Chou et. al.<sup>4</sup>

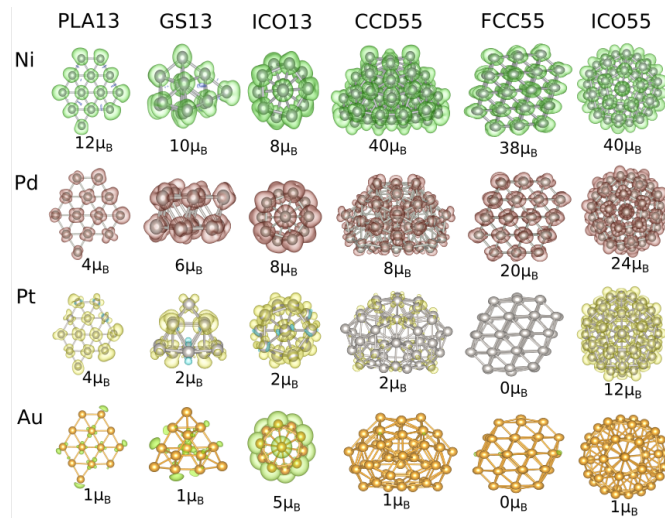


Figure S7: Above are the spin-densities of the gas-phase clusters selected for deposition, with isosurface  $3 \times 10^{-3} e/\text{\AA}^3$ . The gas-phase magnetic moments are shown below the respective clusters.

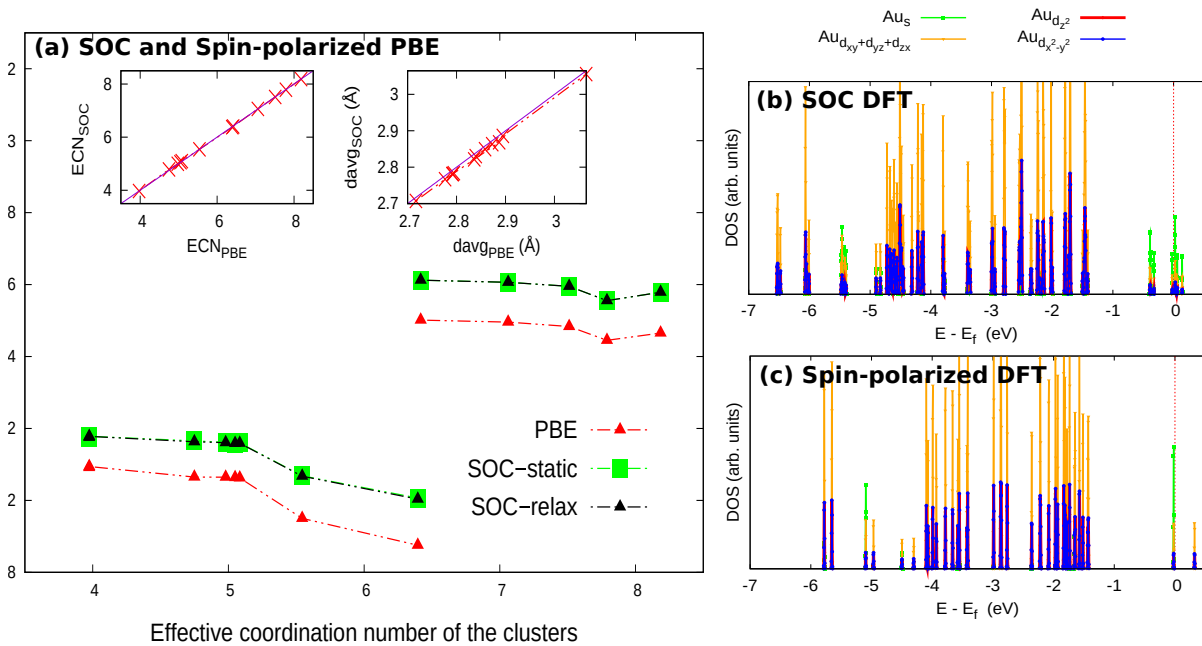


Figure S8: Figure (a) shows the variation of BE for all the isolated Au-clusters for the spin-polarised PBE calculations, SOC-static calculation with the PBE geometry and the relaxed SOC geometry. The inset shows the correlation of  $ECN_{PBE}$  and after relaxing with SOC ( $ECN_{SOC}$ ) on  $y=x$  line. Panel (b) and (c) show the PDOS of Au-ICO<sub>13</sub> cluster for SOC and spin-polarized calculation respectively.

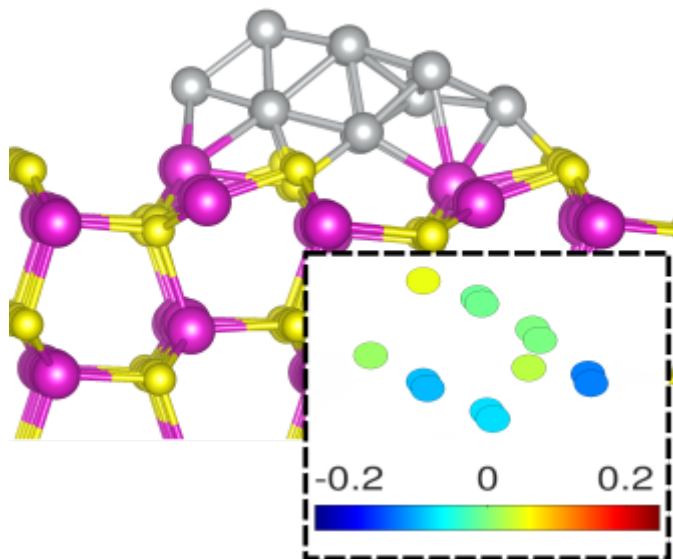


Figure S9: Ni-PLA - stretched input case

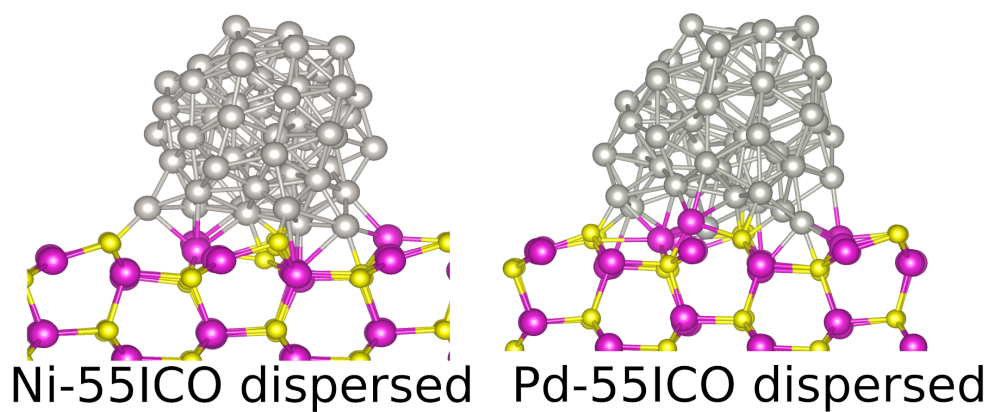


Figure S10: Ni-ICO<sub>55</sub> and Pd-ICO<sub>55</sub> cases derived from a relaxed deposited Pt-ICO<sub>55</sub> configuration.

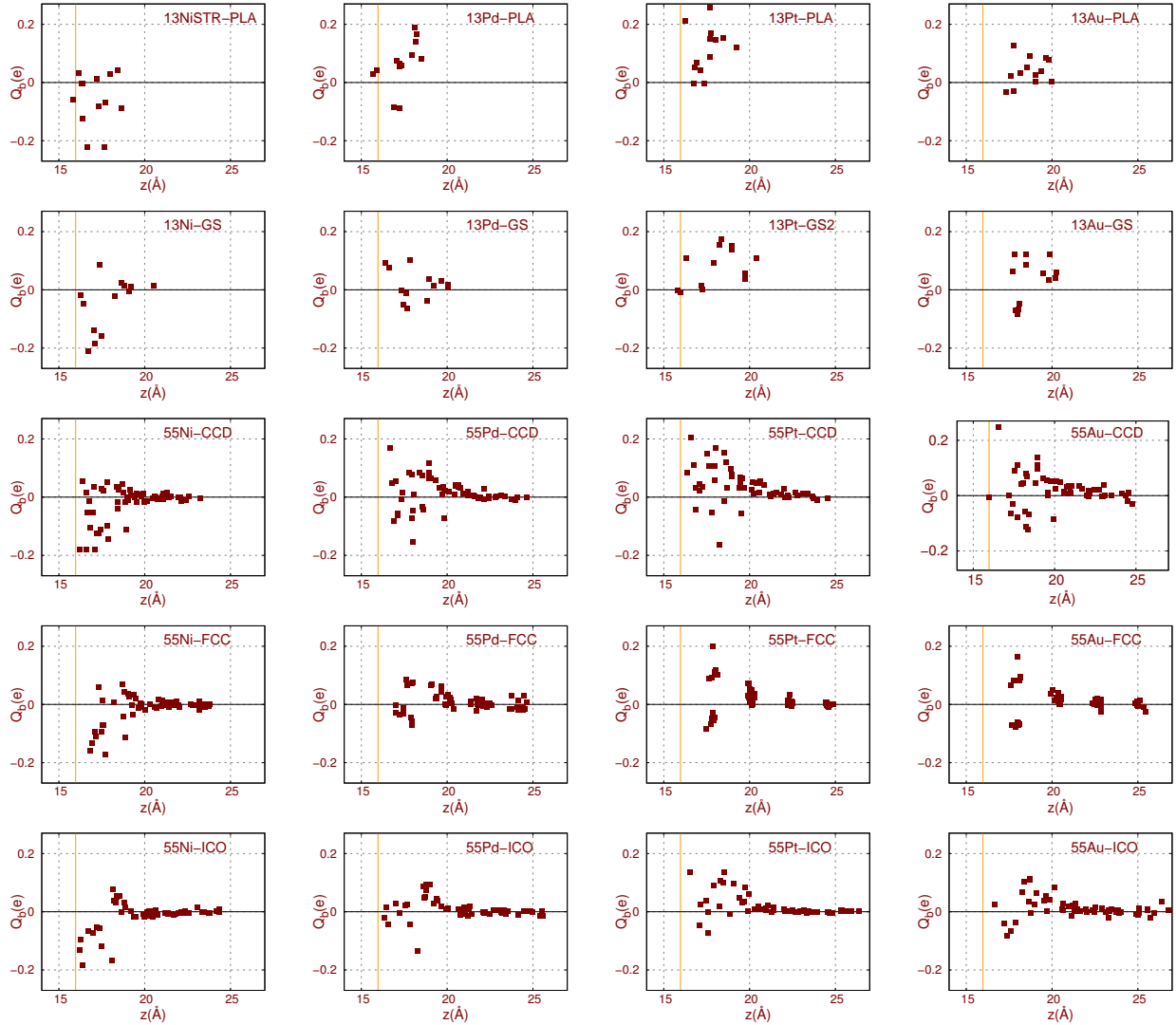


Figure S11: Bader charge difference for metal atom of the clusters,  $Q_M(i)$ , as a function of  $z$ -coordinate of the cell. The dashed line, marks the  $z$ -coordinate of top-layer of the the pristine CdS surface.

## References

- (1) Piotrowski, M. J.; Ungureanu, C. G.; Tereshchuk, P.; Batista, K. E. A.; Chaves, A. S.; Guedes-Sobrinho, D.; Da Silva, J. L. F. Theoretical Study of the Structural, Energetic, and Electronic Properties of 55-Atom Metal Nanoclusters: A DFT Investigation within van der Waals Corrections, SpinOrbit Coupling, and PBE+U of 42 Metal Systems. *The Journal of Physical Chemistry C* **2016**, *120*, 28844–28856.
- (2) Doye, J. P. K. Identifying structural patterns in disordered metal clusters. *Phys. Rev. B* **2003**, *68*, 195418.
- (3) Da Silva, J. L. F.; Kim, H. G.; Piotrowski, M. J.; Prieto, M. J.; Tremiliosi-Filho, G. Reconstruction of core and surface nanoparticles: The example of Pt<sub>55</sub> and Au<sub>55</sub>. *Phys. Rev. B* **2010**, *82*, 205424.
- (4) Chou, J. P.; Hsing, C. R.; Wei, C. M.; Cheng, C.; Chang, C. M. Ab initio random structure search for 13-atom clusters of fcc elements. *Journal of Physics: Condensed Matter* **2013**, *25*, 125305.
- (5) Piotrowski, M. J.; Piquini, P.; Da Silva, J. L. F. Density functional theory investigation of 3d, 4d, and 5d 13-atom metal clusters. *Phys. Rev. B* **2010**, *81*, 155446.
- (6) Pelzer, A. W.; Jellinek, J.; Jackson, K. A. H<sub>2</sub> Reactions on Palladium Clusters. *The Journal of Physical Chemistry A* **2013**, *117*, 10407–10415, PMID: 23980821.
- (7) Sun, Y.; Zhang, M.; Fournier, R. Periodic trends in the geometric structures of 13-atom metal clusters. *Phys. Rev. B* **2008**, *77*, 075435.
- (8) Johansson, M. P.; Warnke, I.; Le, A.; Furche, F. At What Size Do Neutral Gold Clusters Turn Three-Dimensional? *The Journal of Physical Chemistry C* **2014**, *118*, 29370–29377.
- (9) Munoz, F.; Varas, A.; Rogan, J.; Valdivia, J. A.; Kiwi, M. Au<sub>13</sub>-nAg<sub>n</sub> clusters: a remarkably simple trend. *Phys. Chem. Chem. Phys.* **2015**, *17*, 30492–30498.